Liquid Crystals
Publication details, including instructions for authors and subscription information:
http://www.informaworld.com/smpp/title~content=t713926090

Isolation techniques for long-term bistability of the bistable twisted nematic mode

E. J. Acosta[a]; N. J. Smith[a]; M. J. Towler[a]
[a] Sharp Laboratories of Europe Ltd., Edmund Halley Road, Oxford Science Park, Oxford, OX4 4GB, UK

To cite this Article Acosta, E. J. , Smith, N. J. and Towler, M. J.(2006) 'Isolation techniques for long-term bistability of the bistable twisted nematic mode', Liquid Crystals, 33: 3, 249 — 256
To link to this Article: DOI: 10.1080/02678290600583524
URL: http://dx.doi.org/10.1080/02678290600583524

Liquid Crystals, Vol. 33, No. 3, March 2006, 249–256

Taylor & Francis
Taylor & Francis Group

Isolation techniques for long-term bistability of the bistable twisted nematic mode

E.J. ACOSTA, N.J. SMITH* and M.J. TOWLER
Sharp Laboratories of Europe Ltd., Edmund Halley Road, Oxford Science Park, Oxford, OX4 4GB, UK

(*Received 2 August 2005; in final form 3 November 2005; accepted 5 November 2005*)

Low power, storage liquid crystal displays are of interest in the foreseeable future in portable applications. The use of a bistable twisted namatic (BTN) mode in a true storage device requires long term bistability of its operating states since it is intrinsically a metastable device. Two novel isolation techniques are described and demonstrated to isolate and stabilize the operating states in a BTN device. Existing limitations are highlighted and further areas for research suggested.

1. Introduction

The bistable twisted nematic (BTN) mode, first described by Berreman and Heffner [1], consists of a cholesteric (chirally-doped nematic) liquid crystal, with a pitch of approximately twice the cell gap, *e.g.* a thickness-to-pitch ratio (d/p) of 0.5, with antiparallel alignment such that a 180° twist state is adopted at zero volts. In this device geometry there exist three accessible states, the 0°, 180° and 360° states, the 180° state being topologically distinct from the other two states.

More generally, for a BTN with surface alignment orientation Φ, three twist states, the (Φ-π), the (Φ) and the (Φ+π) twist states, can be obtained by suitably matching the d/p ratio to Φ. The BTN configuration described by Berreman and Heffner corresponds to Φ=180° (antiparallel alignment), where the 180° state has the disadvantage of being splayed, so, although the 0° and 360° states have less favourable degrees of twist, they can exist in metastable states with minimal splay. The 0° and 360° states can be selected by application and removal of suitable voltages; hence, these two states are referred to as the two operating states of the BTN. The operation of a BTN LCD is shown in figure 1. From a display device point of view the 180° state is an undesirable, non-operating state, as it cannot be selected quickly via the application or removal of a voltage.

2. Stability of the states

The relative energy of the BTN states at zero voltage (0 V), depends on the alignment orientation (Φ), the thickness-to-pitch (d/p) ratio and the surface tilt (θ_p). At zero surface tilt the Gibbs free energy (G_E) of the three twist states (0°, 180° and 360°) at 0 V is as shown in figure 2. The relative energies indicate that typically the 180° state is the energetically favourable state at 0 V (the global energy minimum state), with the two operating states being metastable.

3. Effect of surface tilt (θ_p) on the states of the BTN

Typically, the surface tilt (θ_p) in a BTN tends to be between 2° and 10° (as in STNs in which a high surface tilt prevents the formation of the striped texture). Increasing the surface tilt changes the relative stability of the states, such that at very high surface tilts the 0° state becomes the energetically favoured state, e.g. at θ_p>75° for a d/p range of 0.5>d/p>0.8. This is useful as it makes the stabilization of the 0° state possible within an isolation region. In some instances the increase in surface tilt can prevent the existence of a state altogether; no solution to the Euler–Lagrange equation exists above a certain θ_p for a set d/p value. For example, the 360° state no longer exists at d/p less than ~0.2 when θ_p is greater than 28°; this is not the case for the 180° state, which only ceases to exist at very high surface tilts, e.g. approximately θ_p>89° for d/p>0.8.

4. Isolation/long term bistability

The photomicrograph in figure 3 shows the nucleated 180° and 360° states growing after the removal of all applied voltages in a pixel previously addressed to the 0° state. After approximately 10 s, the pixel is fully in the 180° state.

In normal BTN displays the update frame rate is sufficient to prevent both the onset (nucleation and

*Corresponding author. Email: Nathan.Smith@sharp.co.uk

Liquid Crystals
ISSN 0267-8292 print/ISSN 1366-5855 online © 2006 Taylor & Francis
http://www.tandf.co.uk/journals
DOI: 10.1080/02678290600583524

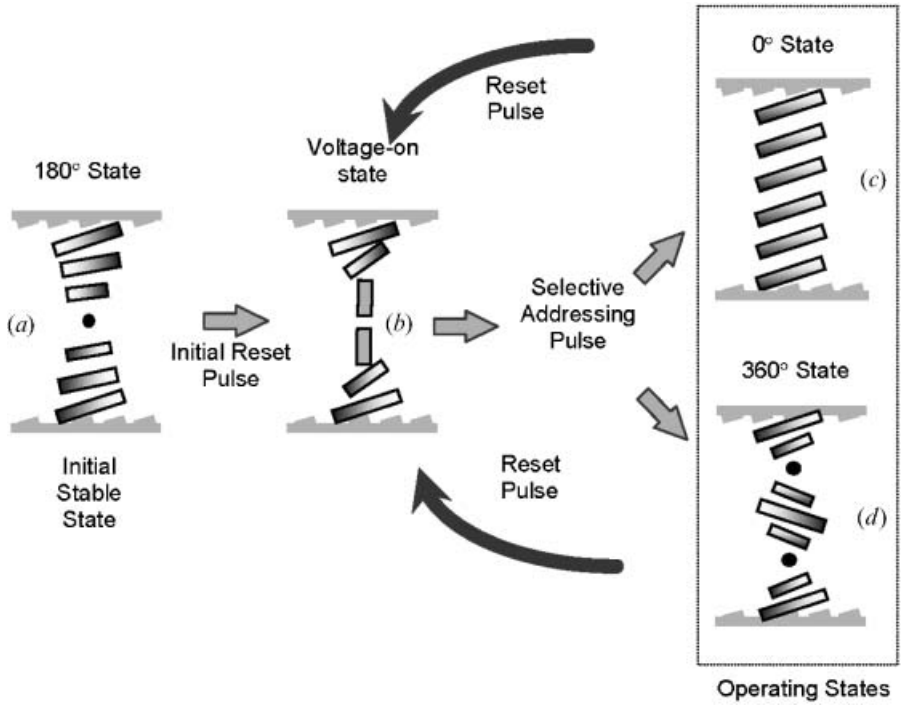

Figure 1. Twist states in a BTN, and its operation. At zero voltage, the initial stable state (*a*) is the 180° state; it is possible to select one of the two metastable operating states, the 0° (*c*) and the 360° (*d*) twist states, via the transition through a voltage-on state (*b*).

growth) of the 180° state and significant growth of the 360° state into 0° state pixels [2, 3]. Alternatively, Nomura *et al*. [4] apply a voltage during a non-select period to maintain the two metastable states. However, low power storage-type displays seek to avoid frequent update; once updated the information remains fixed (at 0 V) until readdressed. Therefore, isolation of the pixels and stabilization of the metastable operating states at 0 V is necessary. Previously suggested isolation methods to stabilize the states in BTNs include:

(1) *Physical barrier*. Hoke and Bos [5, 6] show long-term bistability by forming *in situ* polymer-rich walls around the pixels, isolating and preventing the growth of the unwanted 180° state. Although isolation was demonstrated, well defined wall structures were difficult to obtain, minimizing the active region and aperture ratio of the device. Unlike in actively addressed devices, ionic contamination due to *in situ* polymerization poses less of a problem for passively addressed devices such as the BTN. However, ions, ionic trapping sites

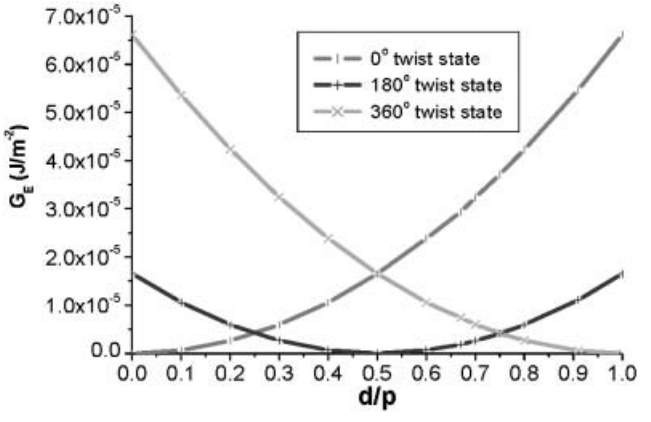

Figure 2. The relative stability of the states as a function of *d*/*p* in a BTN at 0 V with zero surface tilt.

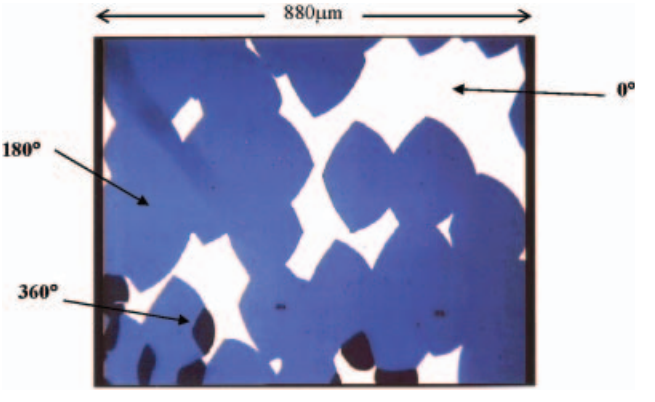

Figure 3. A photomicrograph showing the growth of 360° and 180° states nucleated upon removal of all applied fields within a pixel previously addressed to the 0° state.

and an asymmetric network can result in asymmetric switching. (Positive and negative selection and data pulses result in different switching characteristics.)

(2) *Energy barrier*. Berreman and Heffner [7] describe two isolation methods that aim to stabilize the 0° state within the inter-pixel gaps to form an energy barrier. The first method reduces the cell gap, d, within the inter-pixel gap region to a value that reduces the d/p ratio sufficiently to stabilize the 0° state within it at 0 V. Successful isolation by this method requires a reduction within the inter-pixel gap of ~2/3 and hence compatibility with the cell spacing technique is necessary. The second method increases the surface tilt of both substrates within the inter-pixel gap regions to stabilize a high tilt 0° state at 0 V, as described in § 3. This technique requires a production-compatible fabrication method for patterning of the alignment surface tilt with a high accuracy in the registration of the upper and lower surfaces.

5. Novel isolation techniques

Two novel isolation techniques based on an energy barrier concept are investigated: (1) the twisted hybrid-aligned nematic (T-HAN) isolation technique; (2) the lateral variation in twist (LVT) isolation technique. Each of these isolation techniques establish within the isolation region a state whose configuration is topologically equivalent to that of the higher energy operating state (e.g. the 0° state), thus avoiding the creation of disclinations, and in this way isolating and stabilizing it from the more energetically favourable states. These isolation techniques are achieved by modification (patterning) of the alignment conditions within the isolation regions; be it the patterning of the surface tilt or the alignment orientation. These isolation techniques have the advantage over the Berreman method in that they only require the patterning of one alignment layer, avoiding the need for high registration of upper and lower surfaces.

5.1. *T-HAN isolation technique*

A T-HAN [8] configuration is established within the inter-pixel gaps by providing homeotropic alignment (90°) on one of the surfaces, as seen in figure 4; elsewhere the surface tilt retains a uniform (lower) tilt as required for a BTN. A T-HAN configuration is naturally adopted within the inter-pixel gap under homeotropic–planar alignment, as the LC within the BTN is chirally doped.

A masked rub-down process is used to obtain the required patterned homeotropic–planar alignment. This process is based on a high tilt alignment layer (90° surface tilt) whose tilt can be reduced upon rubbing. The homeotropic alignment is maintained by masking selected regions from the rubbing process, while the unmasked regions are rubbed-down to a uniform low surface tilt, and hence a patterned surface tilt is obtained.

The d/p ratio and the surface tilt (and anchoring energy) of the planar alignment determines the director configuration (twist) adopted within the T-HAN region. As the homeotropic alignment has an undefined azimuthal orientation, the T-HAN can conform to a wide range of twists, including both operating states of the BTN, while acting as an isolation barrier between them. However the T-HAN is topologically non-equivalent to the non-operating (180°) state and hence does not conform to it, with a disclination forming at the interface between them. The conformational properties

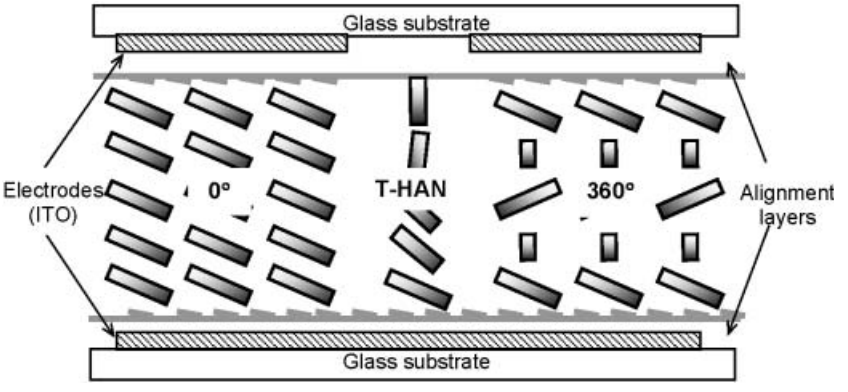

Figure 4. Schematic representation of a T-HAN within the inter-pixel gap isolating both a 0° and a 360° state at 0 V. With the exception of the homeotropic alignment on one of the surfaces within the inter-pixel gap, the surface tilt within the rest of the device is low.

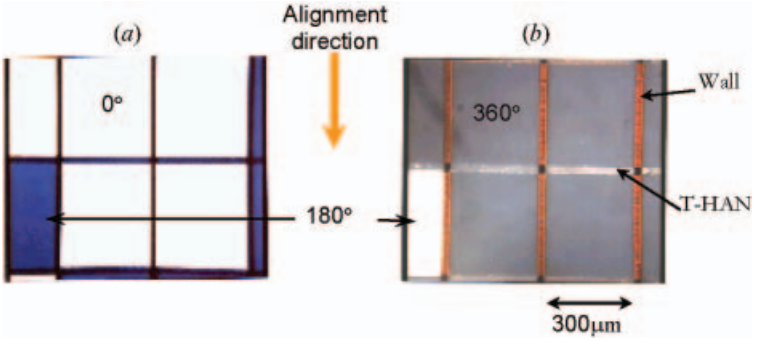

Figure 5. Photomicrographs of T-HAN isolation in a BTN cell at 0 V within the horizontal inter-pixel gaps (light grey), while the vertical gaps contain the cell gap spacer walls (*orange*). For cell details see text.

of the T-HAN are key to its isolation and stabilization properties. Test cells filled with chiral-doped LC mixtures initially consist of the 180° twist state in the active areas separated by regions of T-HAN in the inter-pixel gaps. Application of a voltage removes the 180° twist state and selects the 0° and 360° states.

The T-HAN is found to isolate the 0°, 180° and 360° states successfully. The two photomicrographs in figure 5 show successful isolation of both operating states at 0 V in a BTN cell consisting of $300 \times 300\,\mu m^2$ pixels separated by 30 μm isolation regions with uniform electrodes, cell gap = 2 μm. In figure 5 (*b*), the gain is turned up to differentiate between the vertical and horizontal inter-pixel gaps. No obvious disclinations are observed to exist between the 0° (or the 360°) state and the T-HAN state. The horizontal isolation regions consisted of a T-HAN configuration and the vertical isolation regions consisted of a spacer wall [9]. Long-term isolation of pixels switched into the 0° state, figure 5 (*a*), and the 360° state, 5 (*b*) from the 180° state are observed to remain until readdressed.

The T-HAN isolation was also found to isolate in BTN devices with different cell gaps, e.g. from 1.5 to 10 μm. As the T-HAN functions like a conformational energy barrier, there should exist a limit to the minimum width over which a T-HAN can successfully isolate. Experimentally the minimum isolation (region) width investigated was 30 μm (in a 2 μm BTN cell), which was found to isolate successfully.

It is also an option to pattern the surface tilt alignment of both surfaces in such a way that the patterns complement each other; for example, the isolation regions on the top substrate are made orthogonal to the isolation regions on the bottom substrate, such that the projection of these isolation regions onto one substrate completely surround and isolate the pixels. This patterning (of the surface tilt on both substrates) does not require high levels of registration accuracy in fabrication. An advantage of subjecting both substrates to the same processing steps is a minimization of asymmetry between them that could lead to asymmetric switching characteristics in a BTN LCD due to differing densities/types of ionic trapping sites.

5.2. *LVT isolation technique*

The lateral variation in twist (LVT) isolation technique aims to stabilize a twist state in the inter-pixel gap that can conform (be topologically equivalent) to the higher energy operating state configuration without setting up a disclination, thus isolating it from the lower energy operating state. The alignment orientation within the isolation region is different from that of the active region, hence the twist varies in the lateral direction. Figure 6 shows a schematic representation of a LVT isolation configuration in a BTN. The alignment orientation in the isolation region selects a non-splayed twisted state within it by matching the alignment orientation to both the twist orientation of the LC and the *d*/*p* ratio of the BTN device, such that the twist

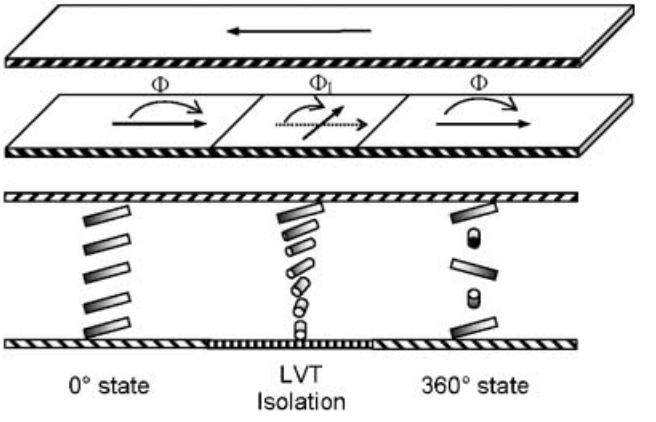

Figure 6. Schematic representation of the LVT isolation in a BTN.

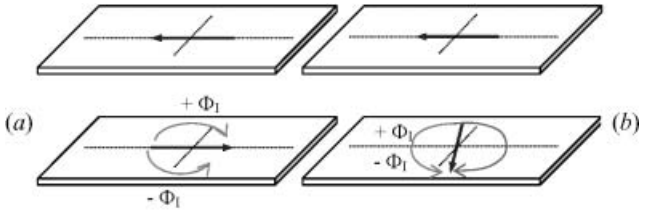

Figure 7. Schematic representations of example orientation angles Φ_I with respect to the rubbing direction in BTN.

state within the isolation region is energetically more stable than that of the 0° state at 0 V.

A suitable twist state (Φ_I) for the LVT isolation region can be determined by satisfying the general expressions (1) and (2) for the *d*/*p* of the BTN under consideration:

$$\left(\frac{\Phi_I}{360}+0.25\right)<\frac{d}{p}<\left(\frac{\Phi_I}{360}+0.75\right) \quad (1)$$

$$\left(\frac{\Phi_I}{360}-0.75\right)<\frac{d}{p}<\left(\frac{\Phi_I}{360}-0.25\right) \quad (2)$$

where Φ_I is the angle between the alignment orientation on the top and bottom substrates within the LVT isolation region, as indicated in figure 7.

The addressable *d*/*p* range for a BTN is approximately 0.57 to 0.82; hence it is this *d*/*p* range which may exist within the isolation region. Expression (1) is utilized to determine the range of orientation angles Φ_I that provide a bend state for this range of *d*/*p* values. The range of orientation angles Φ_I suitable for isolation and stabilization in a BTN is summarized in figure 8 (areas 1 and 2) and table 1. Area 1 corresponds to the combinations of Φ_I-*d*/*p* that should be both addressable and suitable for isolation. Although area 2 is addressable, it may possibly nucleate the 360° state which is favoured by the degree of twist and *d*/*p*. Note that another range of suitable Φ_I will be provided by expression (2) and that for each Φ_I ranges there exists an analogous range for the oppositely twisting *d*/*p*.

The LVT isolation regions are obtained by patterning the alignment layer on one substrate such that the isolation regions have an azimuthal alignment orientation different from that of the rest of the substrate. A masked multi-rub process is used to obtain the required patterned alignment. This process is based on uniformly rubbing the alignment layer to induce one azimuthal alignment direction, providing a first orientation over all the substrate, and then rubbing selected (masked) regions a second time in a different direction to induce a second azimuthal alignment orientation.

BTN cells with different Φ_I in the LVT isolation regions, showed that the LVT isolation technique stabilizes the 0° state at 0 V, while successfully isolating the 360° state from it. Initially, at 0 V the BTN cells contain the 180° twist state in the active pixel regions separated by the LVT isolation regions. The photomicrograph in figure 9 shows the isolation of the 0° from the 360° states within a BTN cell at 0 V (cell gap=6 μm; *d*/*p*~0.69). The LVT isolation regions are 20 μm wide and have a twist of 150°. The 10 μm wide

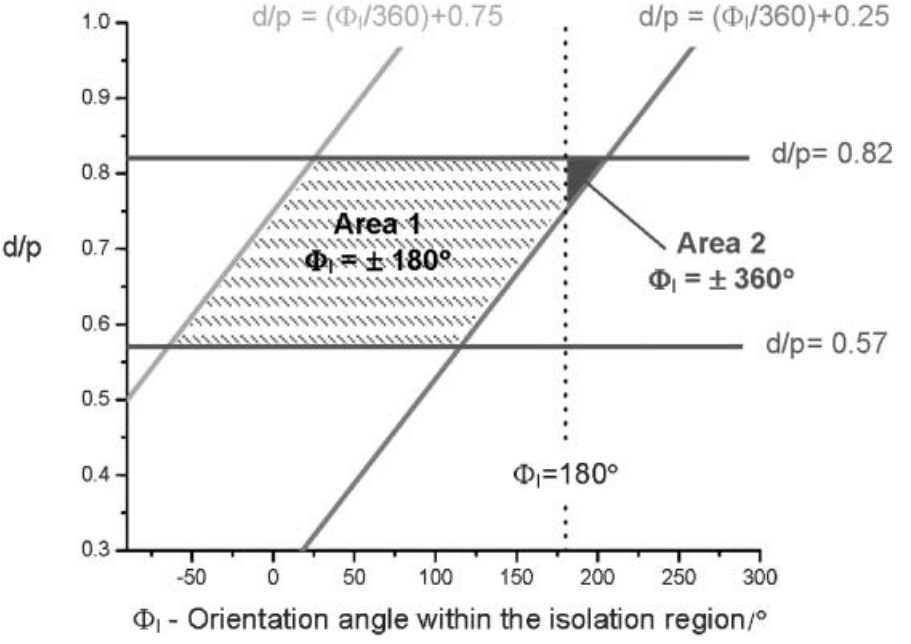

Figure 8. Graph summarizing the range of Φ_I and *d*/*p* that isolate the 0° state in a 0-360° BTN. For explanation see text.

Table 1. Range of Φ_I suitable for isolation in a BTN.

Addressable d/p range		Φ_I range expression (1)	Φ_I range expression (2)
Positive d/p range	+0.57	−64.8° to 115.2°	295.2° to 475.2°
	+0.82	25.2° to 205.2°	385.2° to 565.2°
Negative d/p range	−0.57	−295.2° to −475.2°	−115.2° to 64.8°
	−0.82	−385.2° to −565.2°	−25.2° to −205.2°

isolation regions are found capable of isolation, however they are less reliable, as domains can grow across these narrower isolation regions.

To investigate the effect of different handed chirality, identical cells were filled with left-handed (S811) and right-handed (R811) chiral dopant LC mixtures with a pitch (p) of 10 µm. The LVT BTN cells parameters were: Φ_I=150°, d=6 µm and d/p~0.69. The results are shown in figure 10. It is observed that the d/p - Φ_I combination with the R-dopant stabilizes and isolates the 0° state from the 360° state by forming a 0° state compatible twist state in the isolation region, see figures 10 (*a*) and 10 (*b*) (the 180° state also nucleates, probably from surface defects). On the other hand, it is observed that the d/p - Φ_I combination with the S-dopant stabilizes a 360° state-compatible twist state within the isolation region, figures 10 (*c*) and 10 (*d*), which means that the 0° state is neither stable nor isolated from the 360° state. At 0 V the 360° state proceeds to grow and cover all the area, figure 10 (*c*). These observations agree with expressions (1) and (2), for Φ_I=+150° the R-dopant should be used to obtain successful isolation.

Although the mutual isolation of the 0° and 360° states was successful, the LVT isolation technique was unable to isolate the operating states from the 180° state, see figures 10 (*a*) and 10 (*b*). Hence, successful long-term isolation of the two operating states in a BTN via the LVT isolation technique requires full removal of the 180° state during addressing. A possible reason for the observed failure of the LVT technique to isolate the 180° state at 0 V is the low surface tilt that results from the multi-rub process. Further investigation is required to determine whether this is the main cause.

The photomicrograph in figure 11 shows a magnified image of the BTN cell in figure 9. Observe that no disclination exists between the 0° state and the state within the LVT isolation region, i.e. it appears as a continuous domain. This observation supports the LVT isolation principle, that the isolation state is topologically equivalent to the 0° state and hence able to stabilize it at 0 V. A 2π-disclination line is visible between the 360° state and the state within the LVT isolation region, indicating that the LVT isolation state is unable to conform to the 360° state at 0 V for this particular d/p and Φ_I. The disclination line observed to traverse the 360° domain (in the lower right-hand side) in figure 11 corresponds to a combination of a compressed 0° state and two 2π-disclination lines. This resulted from the growth of a

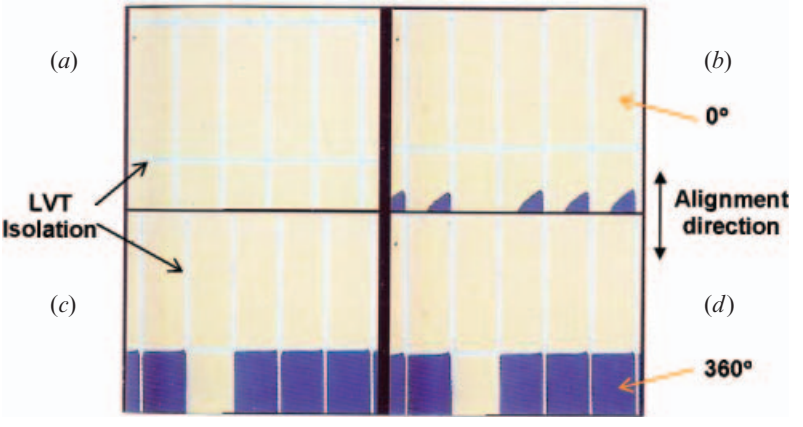

Figure 9. Sequence of photomicrographs of a 6 µm thick BTN cell (d/p~0.69) with LVT isolation, gaps are 20 µm and pixels 200 × 600 µm^2. (*a*) BTN cell at 0 V just after the selection of the 0° state at t=0 s; (*b*) domain growth of the 360° state at 0 V, t~2 s; (*c*) isolation of the 360° state from the 0° state, t~10 s; (*d*) isolation of the 360° state from the 0° state, t~600 s.

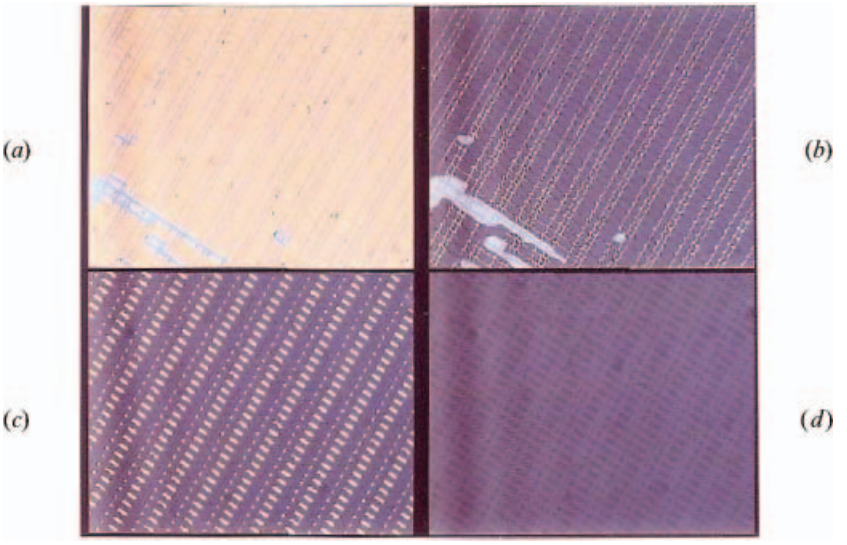

Figure 10. Photomicrographs (× 50) at 0 V immediately after selection of an operating state in a LVT isolated cell (Φ_I=150°, 6 µm thick, d/p~0.69); (*a*) and (*b*) correspond to R811-doped LC, (*c*) and (*d*) to S811 doped LC. The 360° state is selected in (*b*) and (*d*) while the 0° state is selected in (*a*) and (*c*). The inter-pixel gaps are 10 µm and the pixels are $20 \times 40\,\mu m^2$, $40 \times 40\,\mu m^2$ and $80 \times 40\,\mu m^2$.

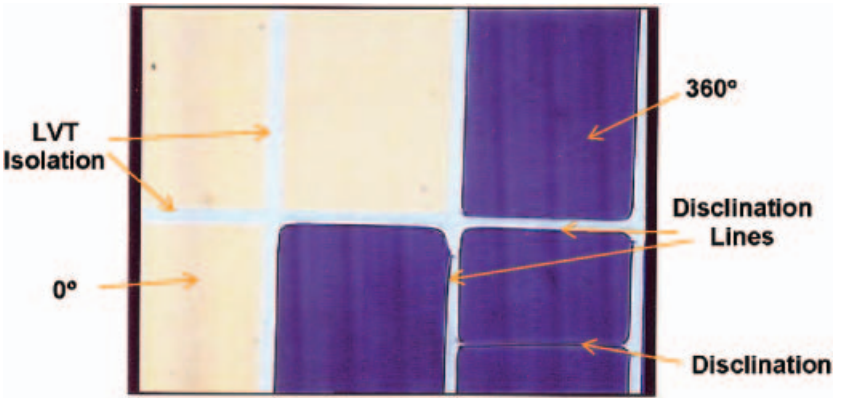

Figure 11. Photomicrograph (× 200) of a BTN (d=6 µm, d/p~0.69) with LVT isolation at 0 V. Gaps are 20 µm and pixels $200 \times 600\,\mu m^2$.

360° state domain from both the top and the bottom ends of the pixel into a pixel that had a 0° state selected within it.

The successful LVT isolation obtained in 6 µm (or thicker) BTN cells could not be reproduced in BTNs with thinner cell gaps of ~2 µm (cell gaps of the order of 2 µm would be required for reflective BTN configurations). The failure to isolate in thinner cell gaps is thought to be due to the elastic energies, which are greater in thinner cell gaps. Further investigations to overcome this include increasing the width of the isolation region while ensuring the surface tilt within the isolation region is much greater than 0°.

6. Conclusion

Two alternative isolation techniques that offer long term stability of a BTN for storage applications are discussed. The T-HAN isolation technique utilizes a patterning of surface tilt while the LVT isolation technique utilizes a patterning of azimuthal alignment orientation; the T-HAN isolation technique is insensitive to the twist orientation of the LC.

Successful isolation and long term stability of the 0° and 360° states were obtained for both techniques in the absence of the 180° state. However, only the T-HAN exhibited successful isolation of the operating states from the 180° state. It is suggested that a possible explanation for the partial failure of the LVT technique

is the low surface tilt that results from the particular fabrication process used. Wider isolation regions may also improve the isolation. The observations suggest the T-HAN to be a more robust isolation technique than the LVT technique.

Suggested future work includes the investigation of the effects of elastic distortion through the cell to determine a minimum isolation width. A more accurate order parameter calculation, to understand the effect of defect energies and surface effects on the isolation capabilities of the isolation region, is also suggested. Finally, the effect of isolation regions and pixel size on the switching characteristics of the BTN should also be characterized.

References

[1] D. Berreman, W. Heffner. EP 0 018 180 (USP 4 239 345) (1980).
[2] C. Hoke, J. Li, J. Kelly, P. Bos. *Jpn. J. appl. Phys.*, **36**, L227 (1997).
[3] C. Hoke, J. Kelly, J. Li, P. Bos. *SID 97 Dig.*, pp. 29–32 (1997).
[4] H. Nomura, Y. Sato, A. Inoue, T. Tanaka, K. Momose. EP 0613 116 A2 (USP 005 684 503 A) (1994).
[5] C. Hoke, P. Bos. *SID 98 Dig.*, pp. 854–857 (1998).
[6] C. Hoke, P. Bos. *IDW '98,* PLC1-1, pp. 201–204 (1998).
[7] D. Berreman, W. Heffner. *J. appl. Phys.*, **52**, 3032 (1981).
[8] E.J. Acosta, M.J. Towler. JP 2 000 338 494 (2000).
[9] P.T. Kazlas, D. McKnight, K. Johnson, S. Gilman. *SID 97 Dig.*, pp. 877–880 (1997).